Academic Journal of Nawroz University (AJNU), Vol.10, No.3, 2021

https://doi.org/10.25007/ajnu.v10n3a1087

CREEP COMPLIANCE OF VISCOELASTIC MATERIALS AT CONSTANT TEPERATURE

Abdulamir S. Resen [1], C. P. Buckley [2]
[1] Engineering College, Nawroz University - Duhok – Iraq, Kurdistan Region, IRAQ
[2] Oxford University – London - England

ABSTRACT

Experiments were carried out to investigate the separate roles of the hydrostatic and deviatoric components of stress tensor (using the first and the second invariant I_1 and I_2'). The results were expressed in term of stress dependent shear compliance J in the time temperature region of the tests (up to10^4 seconds at $30C^0$, of the α −Relaxation).

J was found to increase in magnitude with increasing both hydrostatic I_1,and deviatoric I_2' components of stress. I_1, caused a shift in the magnitude of J and I_2' caused an increase in J with time. The difference between the shear compliance in creep and recovery was found to decrease with I_1, and increase with I_2'.

All the different effects mentioned above could be rationalized by the idea of the time dependent free volume. If the free volume increases with time by increasingI_2' this could explain the difference in the effect of I_1, and I_2'on J and explain why creep is less than recovery.

Keywords:

1. Introduction

The use of the solid polymeric materials increased rapidly, due to its good mechanical properties and cheap compared with other materials. Experimental studies were done for different kinds of polymers under complex loading programs in one and two dimensions [1,2]. This solid polymer cannot be classified as elastic or viscoelastic liquids, since the mechanical properties of these materials depend on the test conditions (e.g., the rate of application of load, temperature, amount of strain). They are described as viscoelastic materials, which can exhibit creep under small load, while creep is the ability of the materials to extent under the effect of a constant applied load for a given time (Fig. 1.1). This could be expressed mathematically as follows: -

$$J(t) = e_c(t)/\sigma_0 \qquad (1.1)$$

The creep compliance J(t) can be statically defined as the change in strain as a function of time under the application of a constant stress [3].

At a small strain the materials behavior is linear, and at a higher strain the material becomes non-linear (Fig. 1.2). This lies between 0.2-0.5%. The Behaviour of the material could be described by applying the Boltzmann Superposition Principle [4] for any complex sequence of stress.

$$e(t) = \int_{-\infty}^{+\infty} J(t-u)\frac{d\sigma}{du}du \qquad (1.2)$$

In the non-linear viscoelastic range, it is difficult to predict the polymer Behaviour. The deviation from the straight line (Isochronous creep curve) demonstrates the non-linearity for the material. The departure will occur beyond a certain strain. This implies that the superposition principal no longer applies.

Any departures from linear viscoelastic behavior are of considerable importance in engineering design, where the design strain for plastic components often lies outside the linear range. In the non-linear range, when values are often imprecise, creep data is used to solve the problem. In practice this problem can be solved satisfactorily by the use of the creep data (Fig.1.3).

After un loading a time dependent recovery is observed (Fig. 1.1). The removal of load could be

modeled as a continuous stress σ, for a time t which is greater than the creep time t_1, where a negative stress - σ, was added (Fig. 1.2). the response to a positive σ, at a time t is

$$e_r(t-t_1) = \sigma\, J(t-t_1) \qquad (1.3)$$

Experimental work was caried out to measure creep and recovery in tension and torsion and combined tension-torsion to find the effect of loads on the solid polymeric materials [5]. In this work the Behaviour of the solid polymeric materials was studied using the creep compliance J for various stress I_1 and I_2' at a constant temperature. The two invariants I_1 and I_2' influence the shear compliance J quite differently. Increasing I_1 cause an almost uniform shift of J versus log time, while increasing I_2' cause increasing separation of the curve with increasing creep time, over 10^4 seconds.

2. Doolittle Equation Concept

The Free-Volume concept is adopted to explain the viscoelastic behavior of PMMA due to the stress applications. This concept was applied by Doolittle [6], and found to represent with high accuracy viscosities of ordinary liquid of low molecular weight

$$\eta_0 = \ln A + b(v - v_f)/v_f \qquad (2.1)$$

Where η_0 is the viscoelasticity, A *and* b are empirical constants, v the specific volume, v_f the specific free volume (Fig. 2.1).

Equation (2.1) implies that the free-volume is the only parameter in determining the rate of the molecular rearrangement and transport phenomena such as diffusion and viscosity which depend on them.

One application of the Doolittle Equation to the WLF [7] equation (2.2), which describes the effect of changing temperature on the shift factor a.

$$\log a = -\frac{b}{2.303\, f_0}\left[\frac{(T-T_0)}{(f_0/\alpha_f)+(T-T_0)}\right] \qquad (2.2)$$

where a, is the time-temperature dependent shift factor, T_0 is a generalized reference temperature, α_f is the expansion coefficient of the free volume, f_0 is the fractional free volume in the reference state.

From equation (2.1) which could be expressed in terms of the shift factor a and free volume factor f, where as $f = v_f/v$

$$\ln a = b\left(\frac{1}{f} - \frac{1}{f_0}\right) \qquad (2.3)$$

The free-volume concept is applied in this work to interpret the non-linear viscoelastic behavior of polymeric materials under stress application, in terms of free-volume.

Assuming that fraction α of the dilation Δ appears as free-volume

$$f = f_0 + \alpha(\Delta - \Delta_0) \qquad (2.4)$$

From equations (2.3) and (2.4)

$$\ln a = \frac{b}{f_0\left[1+\alpha\frac{(\Delta-\Delta_0)}{f_0}\right]} - \frac{b}{b_0} \qquad (2.5)$$

Expanding equation (2.5)

$$\ln a = \frac{-b\alpha}{{f_0}^2}\left[(\Delta-\Delta_0)\ldots\ldots\ldots\frac{\alpha}{f_0}(\Delta-\Delta_0)^2 + \ldots\ldots\right] \qquad (2.6)$$

Where Δ is the dilation

As the dilation difference $(\Delta - \Delta_0)$ is small, equation (2.6) was approximated

$$\ln a = -\frac{b\alpha}{{f_0}^2}((\Delta-\Delta_0) \qquad (2.7)$$

Where a is the shift factor at relaxation time (it is applied at each instant), the value of f_0 = 0.0275, b = 2.12 gives α = 0.9 [8]. The second order curvature in equation (2.6) is not enough to explain the curvature of the shift factor versus the dilation (Fig. 2.2). The shift factor was determined by measuring the shear Compliance J_0 (B, Figure 2.3) at time 10^4 seconds for the smallest applied stress level ($\sigma = 5.477 Mn/m^2$) and a horizontal move for the corresponding value of J on the higher stress level (A, Fig. 2.3) at a different time (lower time). Interpolation was done to find the value of J and the time t' (Fig.2.3).

The dilation Δ was determined for the axial and lateral strains (equation 2.8).

$$\Delta = (e_1 + 2e_2) \qquad (2.8)$$

Where e_1 is the axial strain and e_2 is the lateral strain. The average dilation Δ_{av} was taken for the time $10\ to\ 10^4$ seconds. The departure from linearity suggests that all changes are consistent with time dependent volume change (Fig. 2.2).

3. Time Varying Dilation

Supposing the non-linearity hypothesis, but the free volume is time dependent, let J_0 correspond to the reference state (i.e the initial state). Then assuming that stress effect acts through the time scale (Morland and Lee [9].

$$J(t) = J_0(\eta) \qquad (3.1)$$

Where

$$\eta = \int_0^t \frac{dt'}{a} \qquad (3.2)$$

and η is reduced time (equivalent time in the new state of the material).

The change of the dilation Δ gives a change in the time shift factor a which means Δ is time dependent.

$$\frac{dJ}{dt} = \frac{1}{a}\frac{dJ_0}{d\eta} \qquad (3.3)$$

In terms of the data plotted in (linear – log) (Fig.3)

$$\frac{dJ}{dlogt} = \frac{dJ}{dt}\ \frac{dt}{dlogt} \qquad (3.4)$$

$$\frac{tdJ}{dt} = \frac{tdJ_0}{d\xi}\ \frac{d\xi}{dt} \qquad (3.5)$$

$$t\frac{dJ_0}{d\xi}\frac{1}{a} = \frac{t}{a}\ \frac{adJ_0}{dlog\xi}\ \frac{1}{\xi} \qquad (3.6)$$

$$\therefore\ a^{-1} = \frac{1}{t}\ \frac{dJ}{dlogt} \Big/ \frac{1}{\xi}\ \frac{adJ_0}{dlog\xi}\ \frac{1}{\xi} \qquad (3.7)$$

N. B if a is constant then

$$\frac{1}{a} = \frac{\xi}{t} \qquad (3.8)$$

$$\frac{dJ}{dlogt} = \frac{dJ_0}{dlog\xi} \qquad (3.9)$$

But if $(1/a)$ is increased (e.g due to an increase in dilation with time) then

$$\frac{1}{a} > \frac{\xi}{t} \qquad (3.10)$$

$$\therefore 1 > \frac{dJ_0(\xi)}{dlog\xi} \Big/ \frac{dJ(t)}{dlogt} \qquad (3.11)$$

Consider that means on a $\xi \sim t$ diagram (Fig.3)

$$\frac{1}{a} = \frac{d\xi}{dt} \qquad (3.12)$$

The increase in the dilation Δ_{av} will have the effects

a) $\frac{1}{a}$ increases hence $< \frac{1}{a} >$

b) The shear compliance J will obey equation (3.11).

where $< \frac{1}{a} >$ is the time average reciprocal shift factor.

4. Results and Discussion

Combination of tensile and shear stresses were used, in a set of experiments the first and second invariants (I_1 and $I_2{}'$), I_1 was kept constant and $I_2{}'$ was increased by changing the shear stress τ for each experiment.

The load application was extended to cover the non-linear region. These experiments were started by uniaxial tensile stress, then the shear stress applied, and increased in each experiment using the first and second invariants I_1 and $I_2{}'$ (Fig. 4.1).

Three strains were measured (Axial tensile, Lateral, and Shear strains) in each experiment where biaxial stress was applied.

There is no significant tensile strain, when only shear stress (τ) is applied, (Fig. 4.2 and 4.3). The effect of the tensile shear stress on the compliance J is shown in figure (4.4) for different tensile stress levels. This shows that J increases with increasing σ and time.

The same effect appears, when I_1 was kept constant and $I_2{}'$ increases for each experiment as shown in figures (4.5, 4.6, 4.7, 4.8, 4.9, and 4.10).

When I_1 was kept constant and $I_2{}'$ increased for each experiment as shown in figure (4.1). The first and second invariants (I_1 and $I_2{}'$) were defined in term of tensile and shear stresses $\sigma, and\ \tau$ respectively

$$I_{2'} = \frac{\sigma^2}{3} + \tau^2 \qquad (4.1)$$

When the only stress applied is σ ($\tau = 0$)

$$I_{2'} = \frac{\sigma^2}{3} \qquad (4.2)$$

$$I_1 = \sigma \qquad (4.3)$$

$$I_{2'} = \frac{{I_1}^2}{3} \qquad (4.4)$$

From equations (4.1, and 4.3) it can be seen that the increase of τ affect $I_2{}'$ only, where the increase of σ affects I_1 and $I_2{}'$. The time dependent deformation of PMMA at room temperature is influenced by the broad β retardation process [10]. This β retardation process is thought to have rotations within side groups which may be coupled to local torsional displacement of the main polymer chain [11].The increase in the shear compliance

J corresponds to the short - time tail of the glass rubber or $\alpha-$ relaxation process which marks the onset of hindered rotation around main - chain bond with consequent rearrangements in local chain conformation [12]. The results of this work are at the beginning of the

$\alpha-$ relaxation process (All tests are carried out at 30^0C).

The effect of increasing I_1 at constant $I_2{}'$ was to produce approximately constant shift in J as shown in figures (4.11, 4.12) and the effect of $I_2{}'$ at constant I_1 was found to produce a separation in shear compliance J with increasing time. With applying shear stress τ only, the shear creep compliance curves shift to a shorter time (with increasing $I_2{}'$ and the absence

of I_1) [13]. The effect of the non-linearity could be due to I_1 at the beginning of the experimental time, where the effect of the non-linearity was due to $I_2{}'$ at a later time. This means that I_1 affects the volume at short time and $I_2{}'$ at long time.

From the results, it was found that the increase of Δ with I_1 is independent of time.

The creep data for each experiment were compared with the recovery data. These creep and recovery data were determined using the Buckley and McCrum approach [14]. It was found that by dividing the shear compliance $J(t, I_1, I_2{}')$ from torque and the shear compliance from the tensile load $[\gamma/\tau][\sigma/2(e_1 - e_2)]$ is always equal to 1 (Fig. 4.13). The result shows the same for recovery were the recoverable shear compliance J_r defined as shown in figure (4.14). The three strains e_1, e_2, and γ are used for recovery to define the shear compliance.

All the experiments used in this work, whether uniaxial or biaxial stress, show recovery compliance always exceeding creep compliance (Fig. 4.15, and 4.16) over the time scale studied. This has been shown by many researchers [15,16].

$$J_r - J_c > 0 \qquad (4.6)$$

The effect of $I_1, and\ I_2{}'$ on $(J_r - J_c)$ is as if the second invariant $I_2{}'$ produces the

non-linearity effect and the first invariant I_1 is to kill this effect.

Because the Doolittle equation works with changing of the temperature, an assumption was made that it could work with changing of the stress (stress inducing dilation). This was done by measuring the shear compliance J and finding the volume change from the uniaxial tensile stress application experiments.

The measurements of the volume changes were established from the uniaxial test only,

because of the difficulties in measuring the changes in the thickness of the specimen when subjected to biaxial stress other than uniaxial tensile stress,

The shift with the volume could be found with the base of the Doolittle equation (2.7) and on the other hand from the experimental data and the changes of the creep curves with volume for the polymeric materials. To find the shift factor, a point on the lowest shear compliance J (B, Fig. 2.3) is taken and an assumption is made that the shift is a horizontal shift only (B shifted by a reduction in the relaxation time is found), the point B is shifted to the point A which is on a higher stress state. To find the point A in figure (2.3) a linear interpolation scheme was applied (Fig. 4.17)

$$\frac{logt'-logt_P}{logt_Q-logt_P}=\frac{J'-J_P}{J_Q-J_p} \qquad (4.7)$$

$$\therefore\ logt'=logt_P+\frac{logt_P-logt_Q}{J_Q-J_P}\left(J'-J_p\right) \qquad (4.8)$$

The shift factor was found by a fit of J with lower stress data of $logt = 4$ to the creep curve for the higher stress level.

The Doolittle equation was found to fit the first five points (Fig. 2.2) very well (with $\alpha = 0.9$), but after that the shift $< 1/a >$ increase more slowly than predicted, but this could be explained by the dilation increasing with time, here $< 1/a > < 1/a$ (Fig. 3). This condition was supported qualitatively by the fact that the J versus $logt$ curves exhibited the trend expressed in equation (3.11).

5. Conclusion

From the results of this work, it can be concluded that the two invariants I_1 and I_2' influence the shear compliance J quite differently. Increasing I_1 cause an almost uniform shift of J versus log time, while increasing I_2' cause increasing separation of the curve with the increasing creep time, over 10^4 seconds.

With increasing I_1 at constant I_2', there was no significant variation to within the scatter 12% for time of 10^4 seconds.

The effect of the invariants on the creep and recovery shear compliances J_c *and* J_r were different. I_2' was found to increase the difference between the creep and recovery shear compliances $\Delta J = J_r - J_c$, where as an increase of I_1 was found to decrease the difference between creep and recovery compliances.

The time independent free-volume theory was applied to the uniaxial tensile data. This theory was found to fit the first five experimental data (fitted the dilation versus the time dependent shift factor).

The time dependent dilation appeared to be enhanced with increasing I_2'. This explains why the experimental data for the four other data points does not appear to obey the Doolittle equation at the end (because the way the graphs where plotted).

The mean features of the results can be explained by the non-linearity being controlled by the volume and the deviatoric stress causing the time dependent dilation.

6. References

1. Buckley C.P., "Multiaxial nonlinear viscoelasticity of solid polymers", Polymer Eng. Sci. Vol. 27, No. 155, 1987
2. Ward, I. M. "Mechanical Properties of Solid Polymers", John Wiley (2nd Edition), 1983
3. Catherine A. et.al. "Contact Creep Compliance of viscoelastic Materials via Nanoindentation" J. Materials. Re., Vol. 21, No. 6, Jun 2006
4. Boltzmann, L. "Super Position Principal of the Beginning Linear Viscoelasticity", Pogg. Ann. Phys. 7, 624, 1957
5. Resen A. S "Biaxial Creep of Plastics", PhD. Thesis, University of Manchester Inst. of Sci. and Tech., England, 1988.
6. Doolittle A. K. "Studies in Newtonian Flow. II. The Dependence of the Viscosity of Liquids on Free-Space", J. Phys. 22, 1471, 1951
7. Williams M. L., Landel, R. F. and Ferry, "The Temperature Dependence of Relaxation Mechanisms in Amorphous Polymers and other Glass-forming Liquid", J. D. Am. Chem. Soc. 77, 3701, 1955
8. Ferry, J. D. Viscoelastic properties of Polymers, John Wily and Sons 1978
9. Morland L. W. and Lee E. H. "Stress Analysis for Linear Viscoelastic Materials with Temperature Variation" Trans. Soc. Rheol., 4, 233, 1960,
10. Read B. E., and Dean G. D. "Time-dependent deformation and craze initiation in PMMA: Volume effects", J. Polymer, 25, 1679, 1984
11. Read B. E. "Influence of stress state and temperature on secondary relaxations in polymeric glasses", J. Polymer Vol. 22, 1580, 1981,
12. McCrum, N. G., Read B. E., and William, G. "Anelastic and Dielectric Effect in Polymeric Solids", John Wiley and Sons, London, 1967.
13. Struik, L. C. E. "Physical Aging in Amorphous Polymers and other Materials", El, Sevier, Amsterdam, 1978
14. Buckley, C. P., McCrum, N. G., "The relation between linear and non- linear viscoelasticity of PP", *J.* Mater. Sci., Vol. 9, PP. *2064*-2066, *1974*. 5.
15. Ward, I. M., and Onat, E. T. "Non-linear mechanical Behaviour of oriented polypropylene", J. Mech. Phys. Solids, Vol. 11, 217, 1963
16. Turner, S. "The strain response of plastics to complex stress histories", J. Polymer Eng. Sci., Vol. 6, 306, 1966

Appendix I

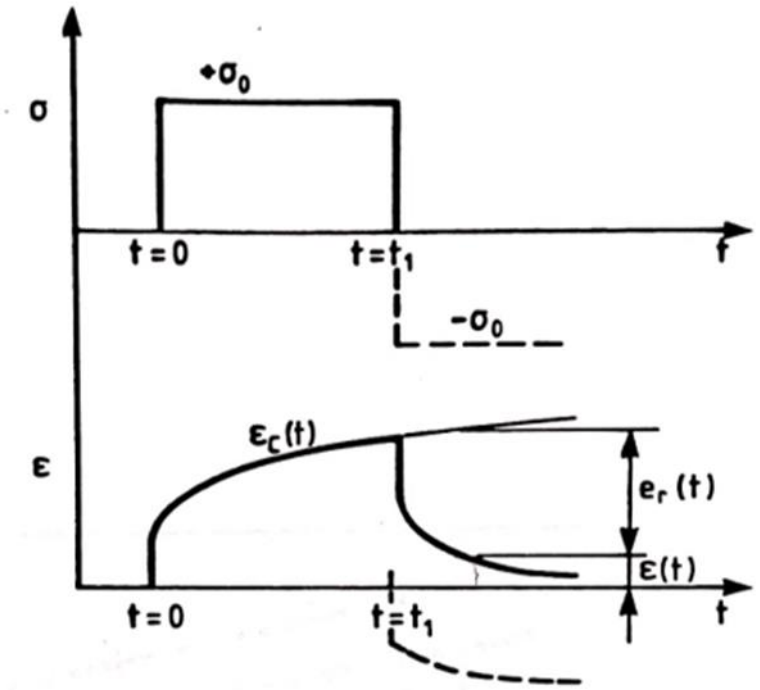

Fig. (1.1) Creep and Recovery under constant Stress schematic diagram

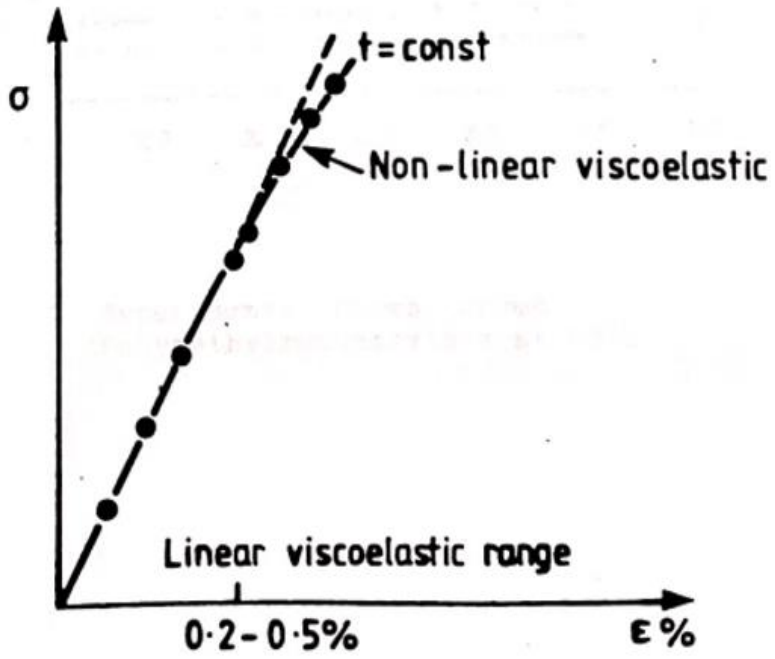

Fig. (1.2) Isochronous Creep Curve

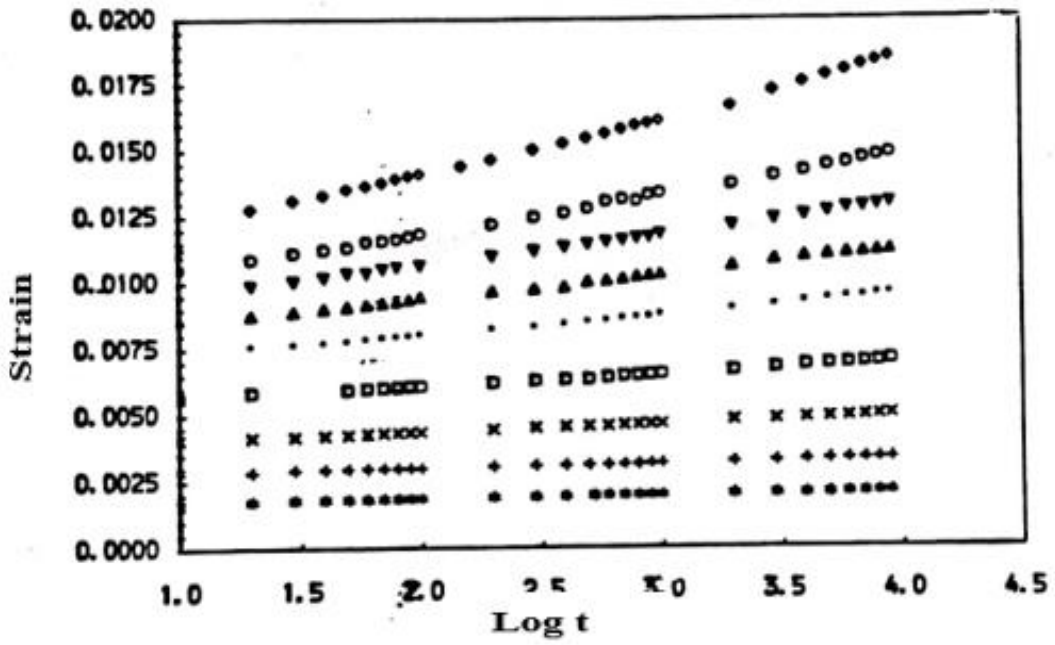

Fig. (1.3) Experimental Creep Curve (polymethylmethacrylate at 30^0C)

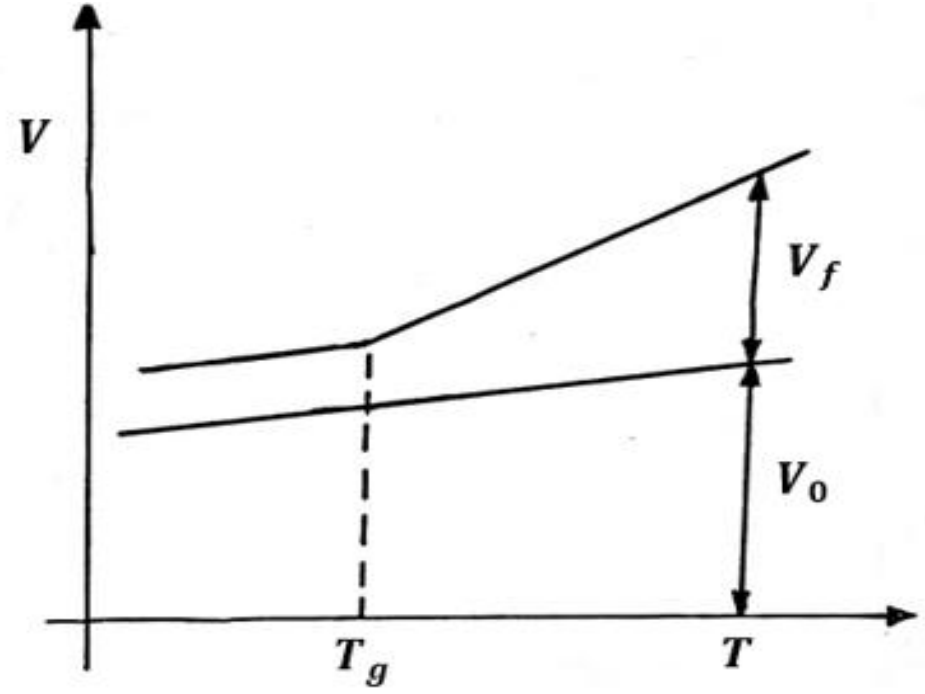

Fig. (2.1) Schematic Diagram for Volume change with Temperature

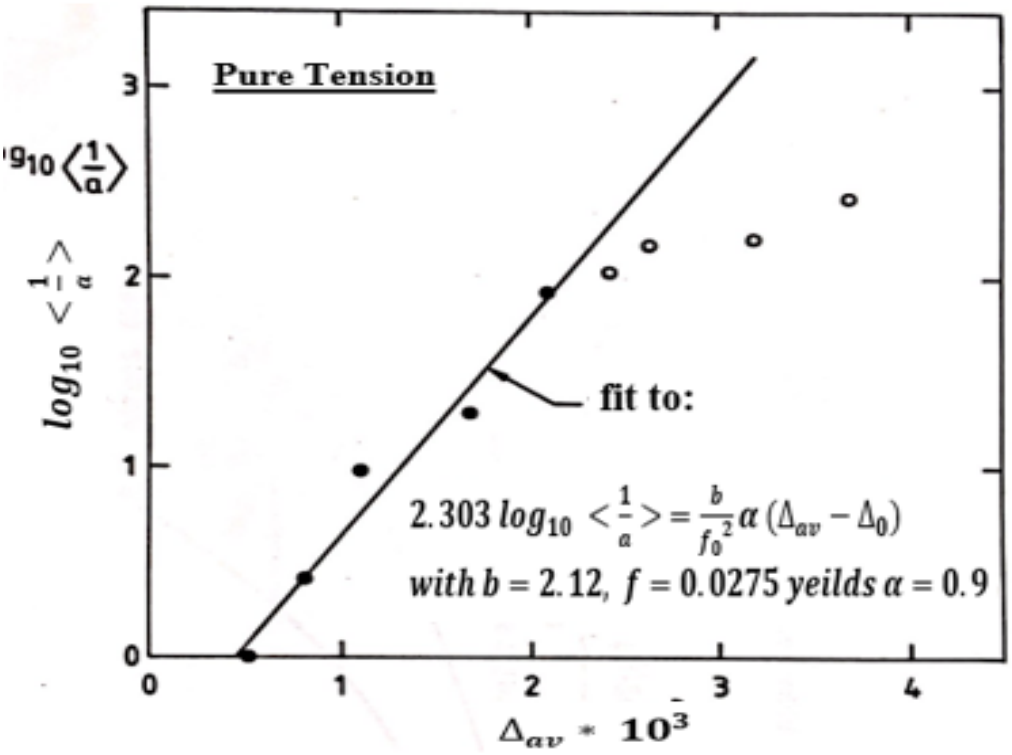

Fig. (2.2) The Shift factor versus the average dilation for different stress level

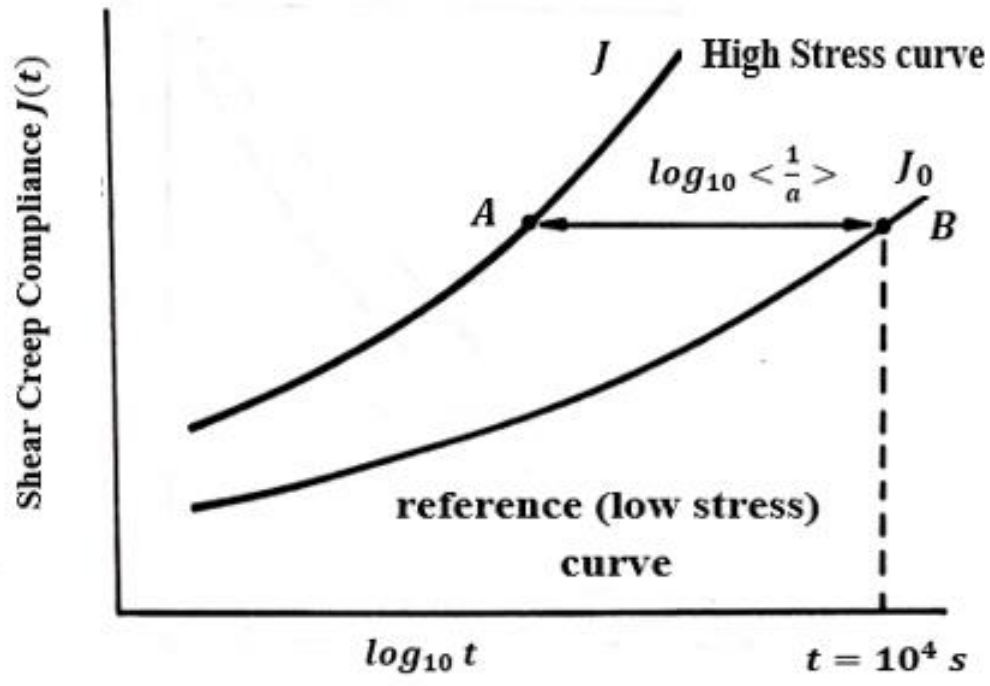

Fig. (2.3) Apparent Shift factor schematic diagram

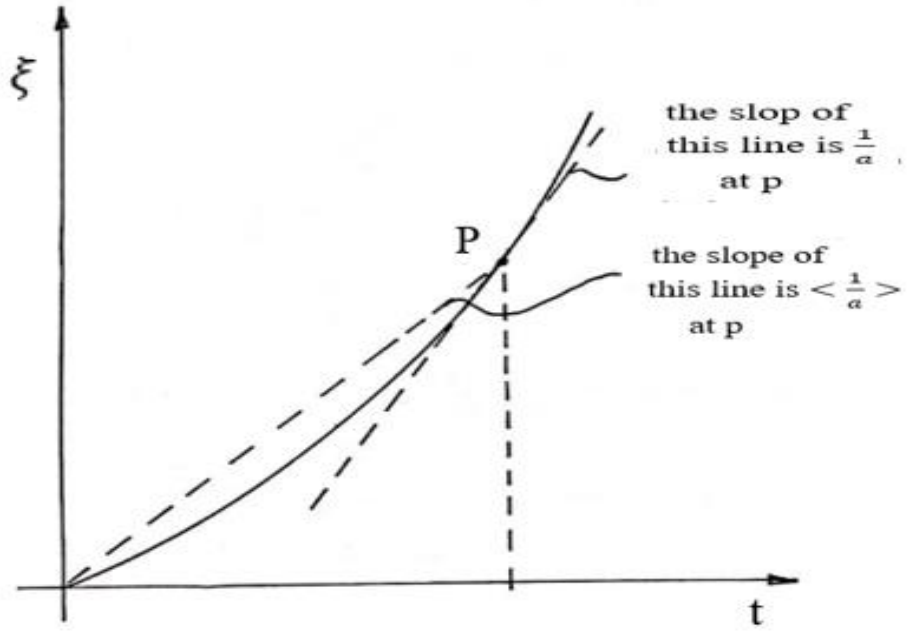

Fig. (3) Equivalent time versus Normal time schematic diagram

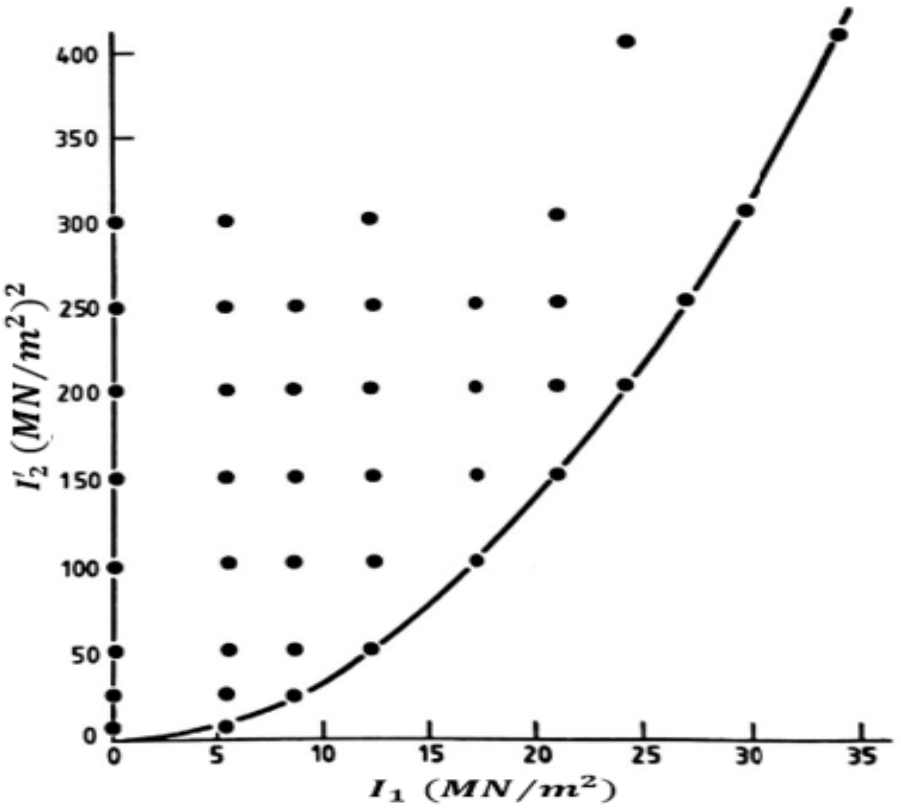

Fig. (4.1) First and second stress invariants I_1 and I_2' space in combined tension-torsion

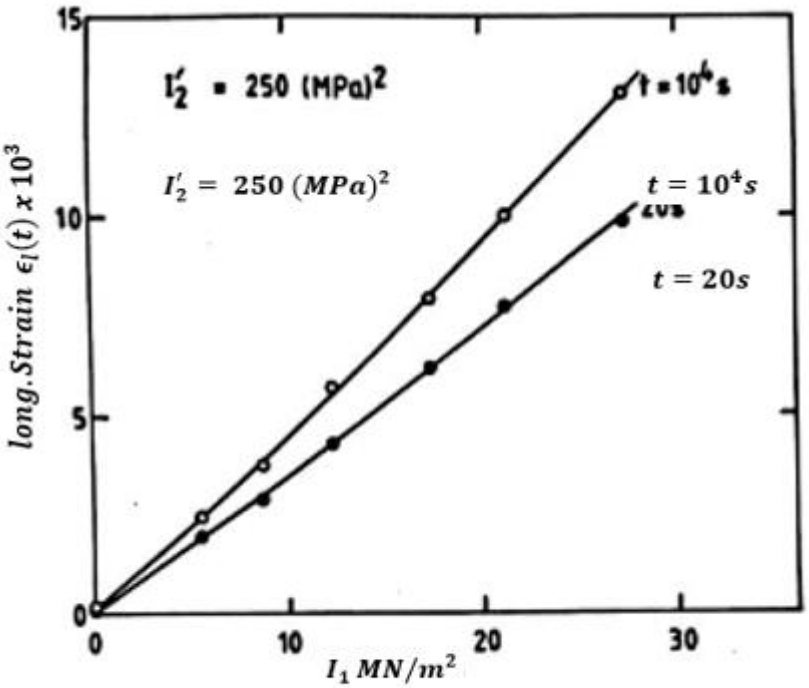

Fig. (4.2) Axial strain versus first invariant I_1 at constant $I_2' = 250\ (MPa)^2$ and time $(t = 20\ to\ 10^4\ seconds)$

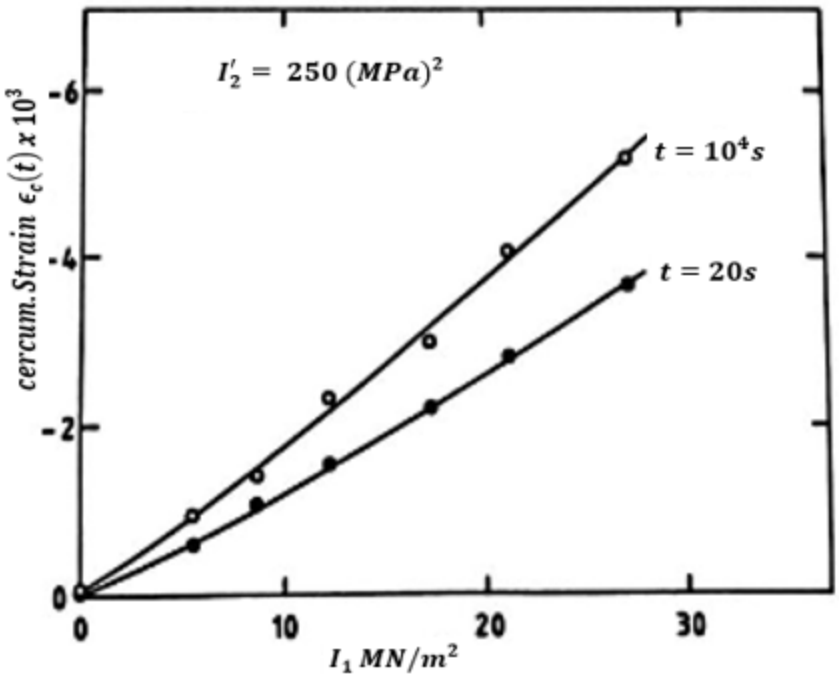

Fig. (4.3) Lateral strain versus first invariant I_1 at constant $I_2' = 250\ (MPa)^2$ and time $(t = 20\ to\ 10^4\ seconds)$

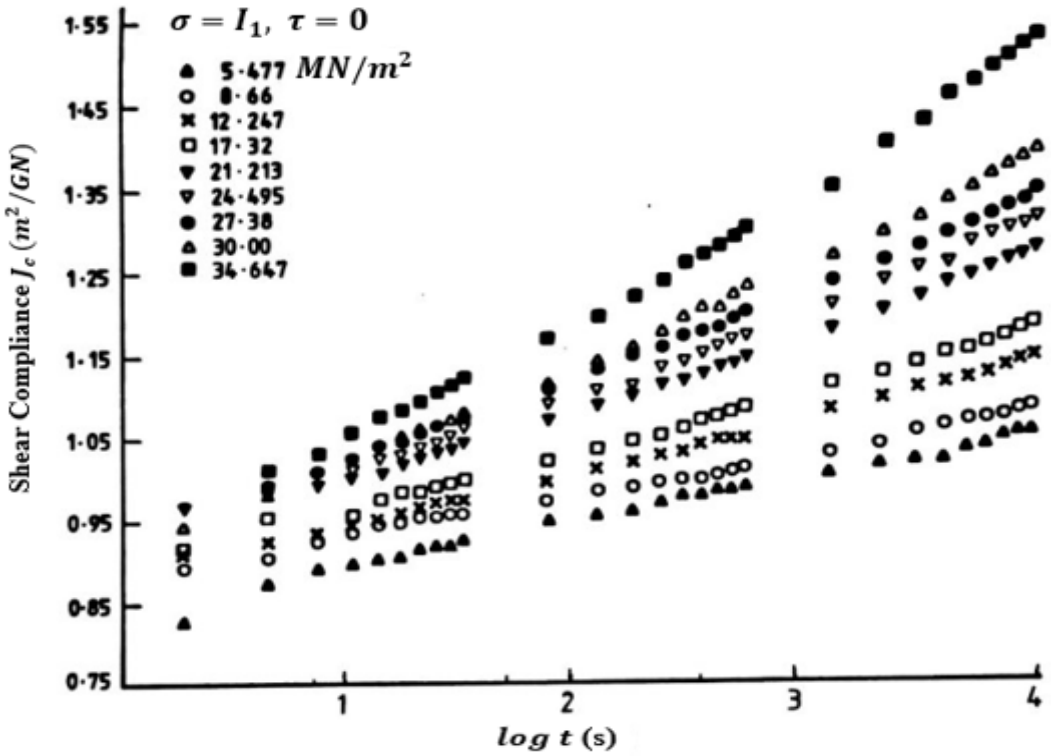

Fig. (4.4) Shear Compliance J_c as a function of time at $\tau = 0$ and varying $\sigma = I_1$ $(T = 30 \pm 0.2C^0)$

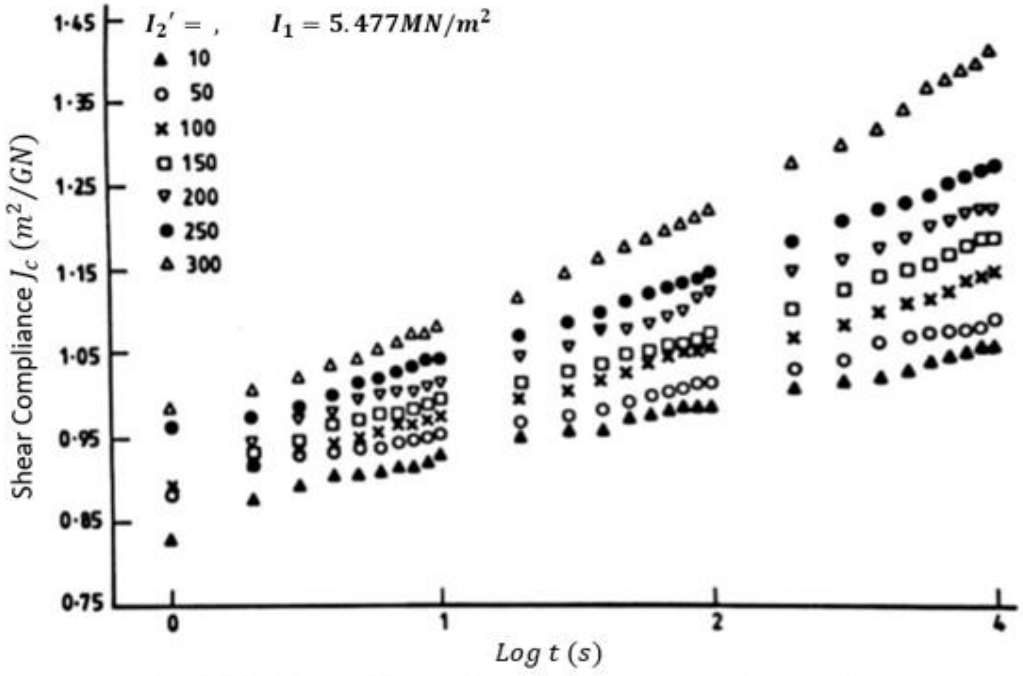

Fig. (4.5) Shear Compliance J_c as a function of time at a constant I_1 and varying I_2' $(T = 30 \pm 0.2C^0)$

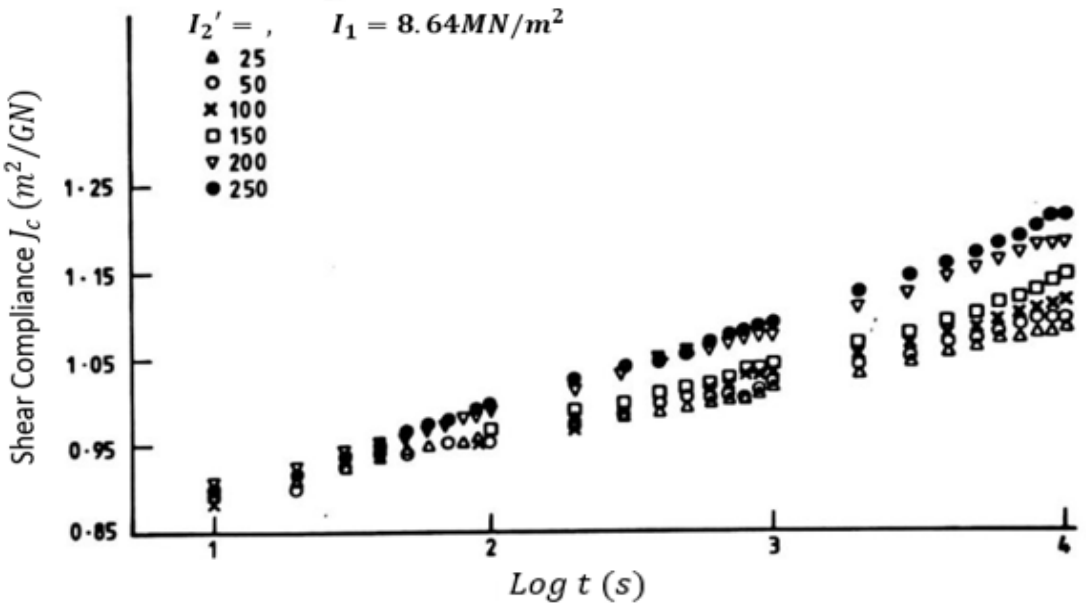

Fig. (4.6) Shear Compliance J_c as a function of time at a constant I_1 and varying I_2' $(T = 30 \pm 0.2C^0)$

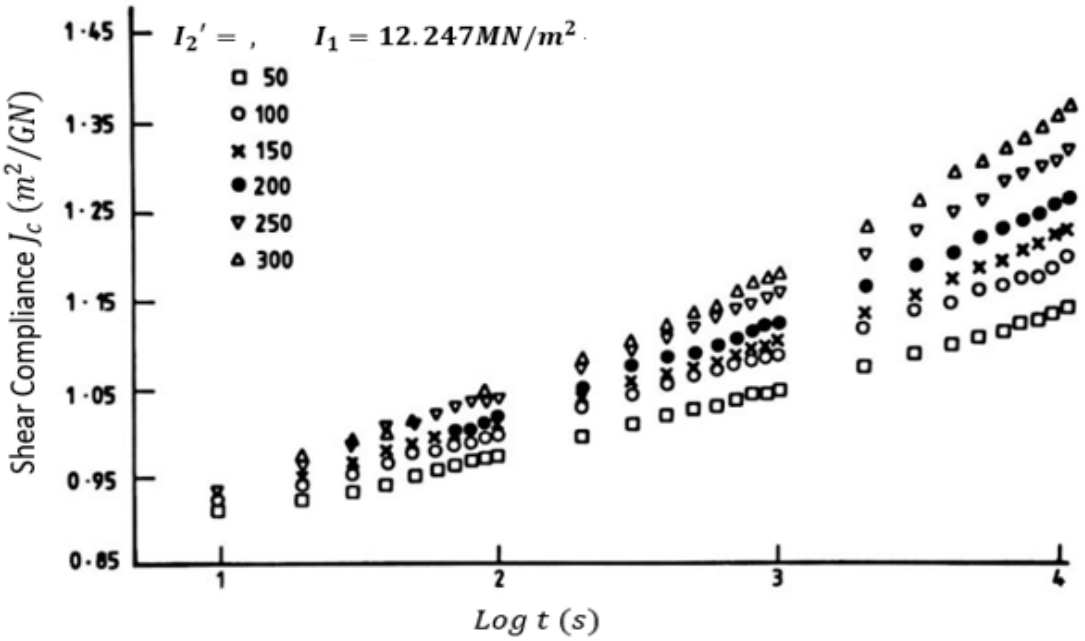

Fig. (4.7) Shear Compliance J_c as a function of time at a constant I_1 and varying I_2' $(T = 30 \pm 0.2C^0)$

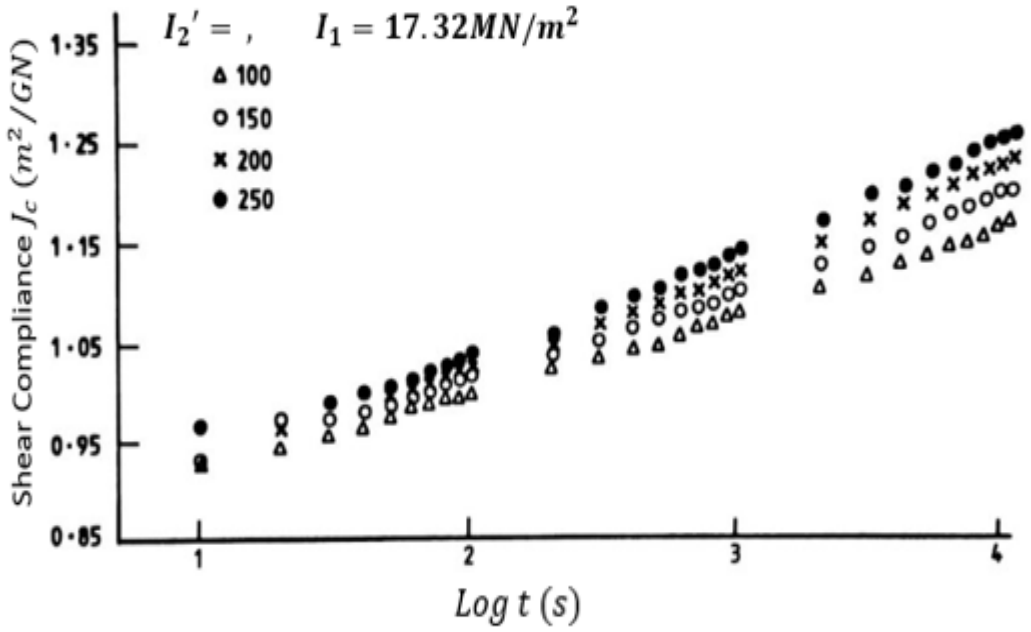

Fig. (4.8) Shear Compliance J_c as a function of time at a constant I_1 and varying I_2' $(T = 30 \pm 0.2C^0)$

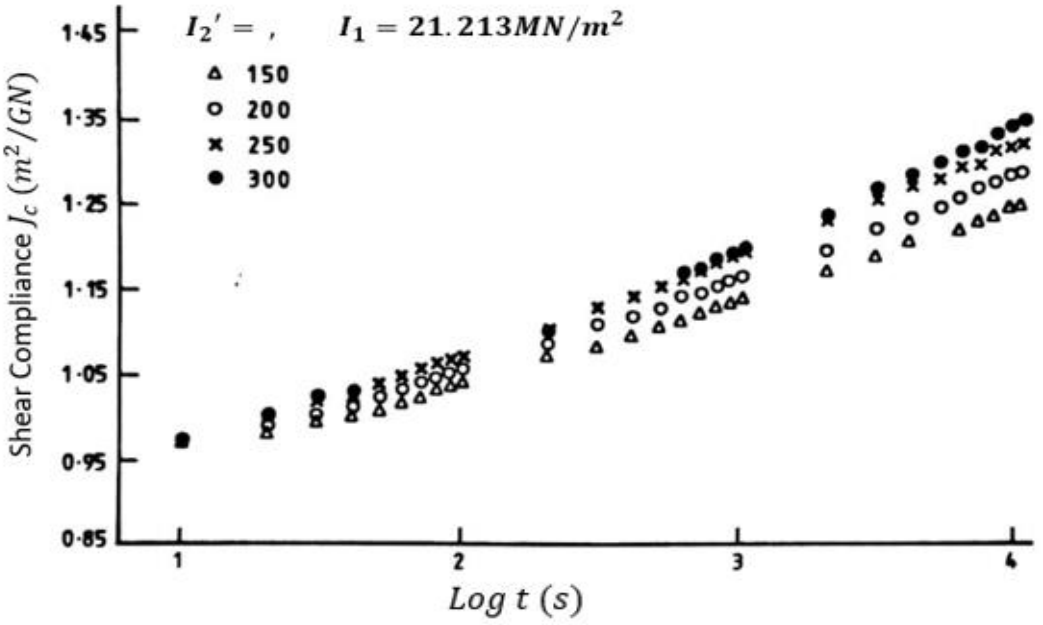

Fig. (4.9) Shear Compliance J_c as a function of time at a constant I_1 and varying I_2' $(T = 30 \pm 0.2C^0)$

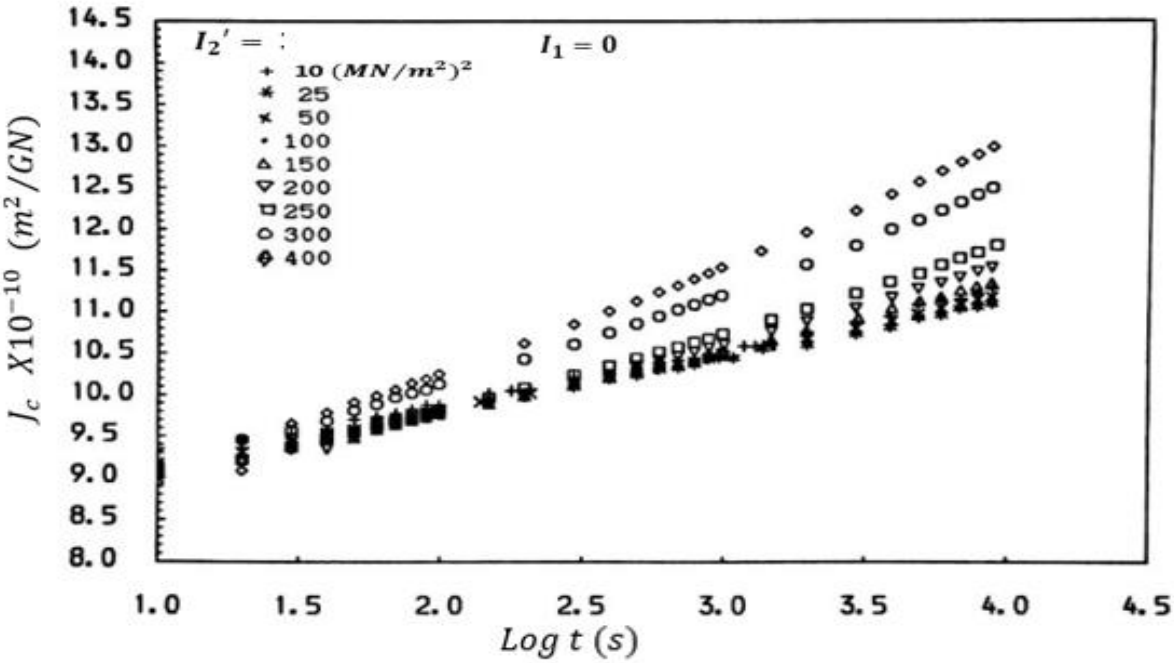

Fig. (4.10) Shear Compliance J_c as a function of time at a constant I_1 and varying I_2' $(T = 30 \pm 0.2C^0)$

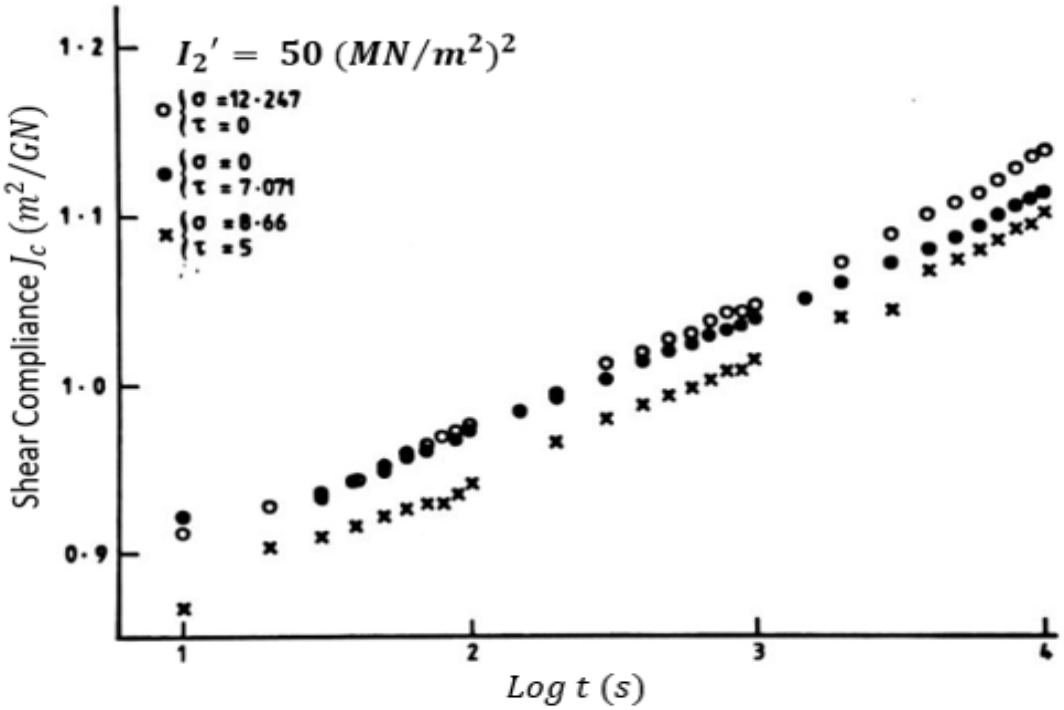

Fig. (4.11) Shear Compliance J_c as a function of time at a constant I_2' and varying I_1 $(T = 30 \pm 0.2C^0)$

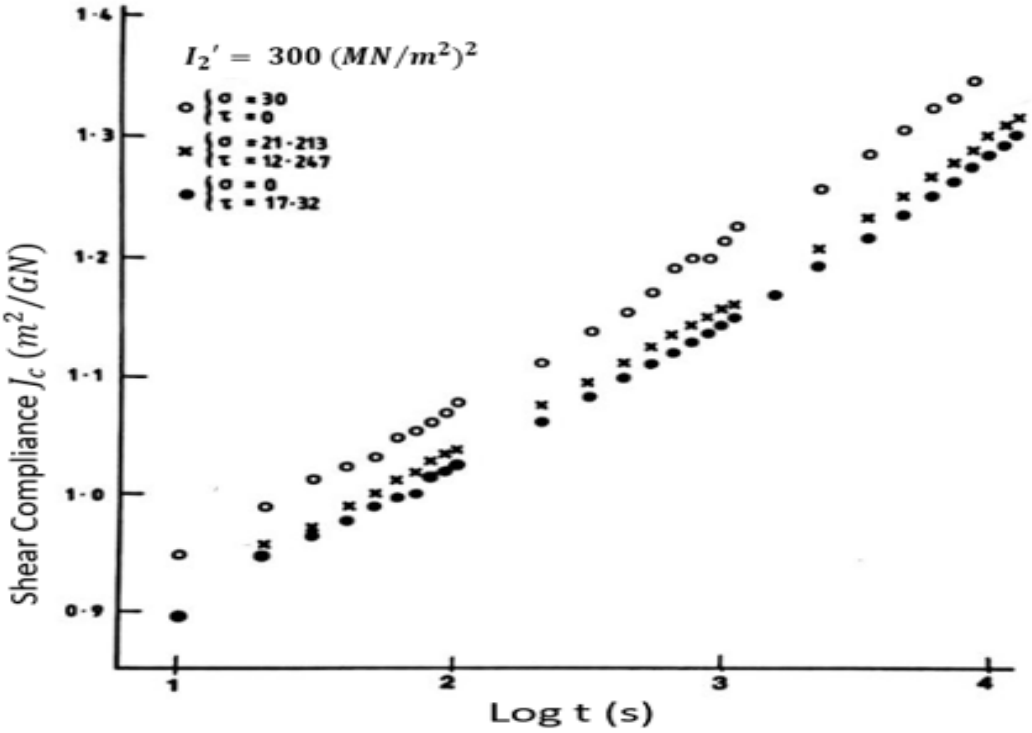

Fig. (4.12) Shear Compliance J_c as a function of time at a constant I_2' and varying I_1 $(T = 30 \pm 0.2C^0)$

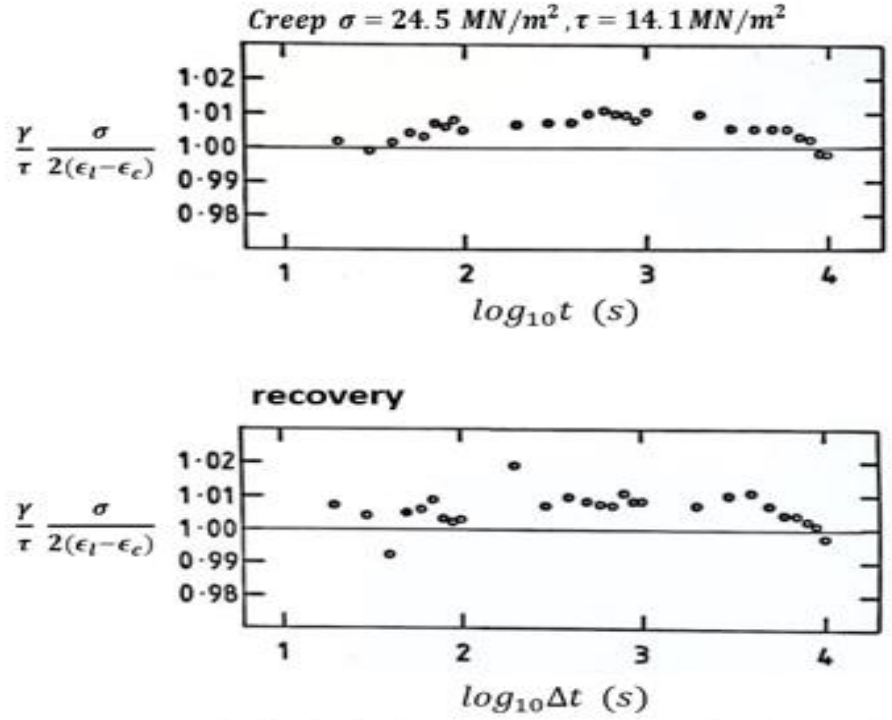

Fig. (4.13) The shear compliance measured from shear strain divided by shear compliance measured from tensile strain, J_γ and J_α under combined tension-torsion for creep and recovery (as function of time).

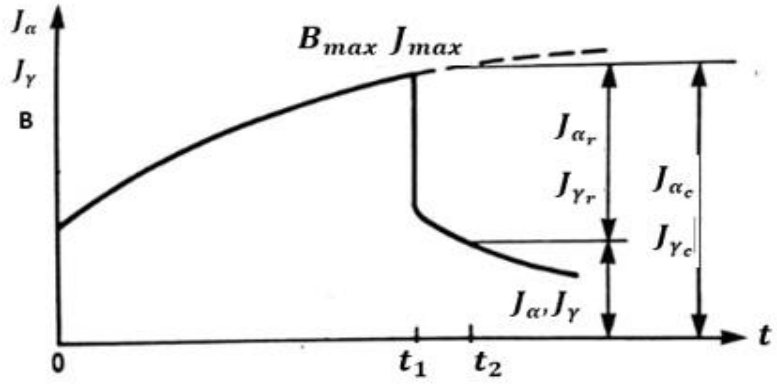

Fig. (4.14) Shear compliance calculated from tensile strains measured from shear strain divided by shear compliance measured from tensile strain, J_α and shear compliance calculated from shear strains J_γ in creep and recovery schematic diagram

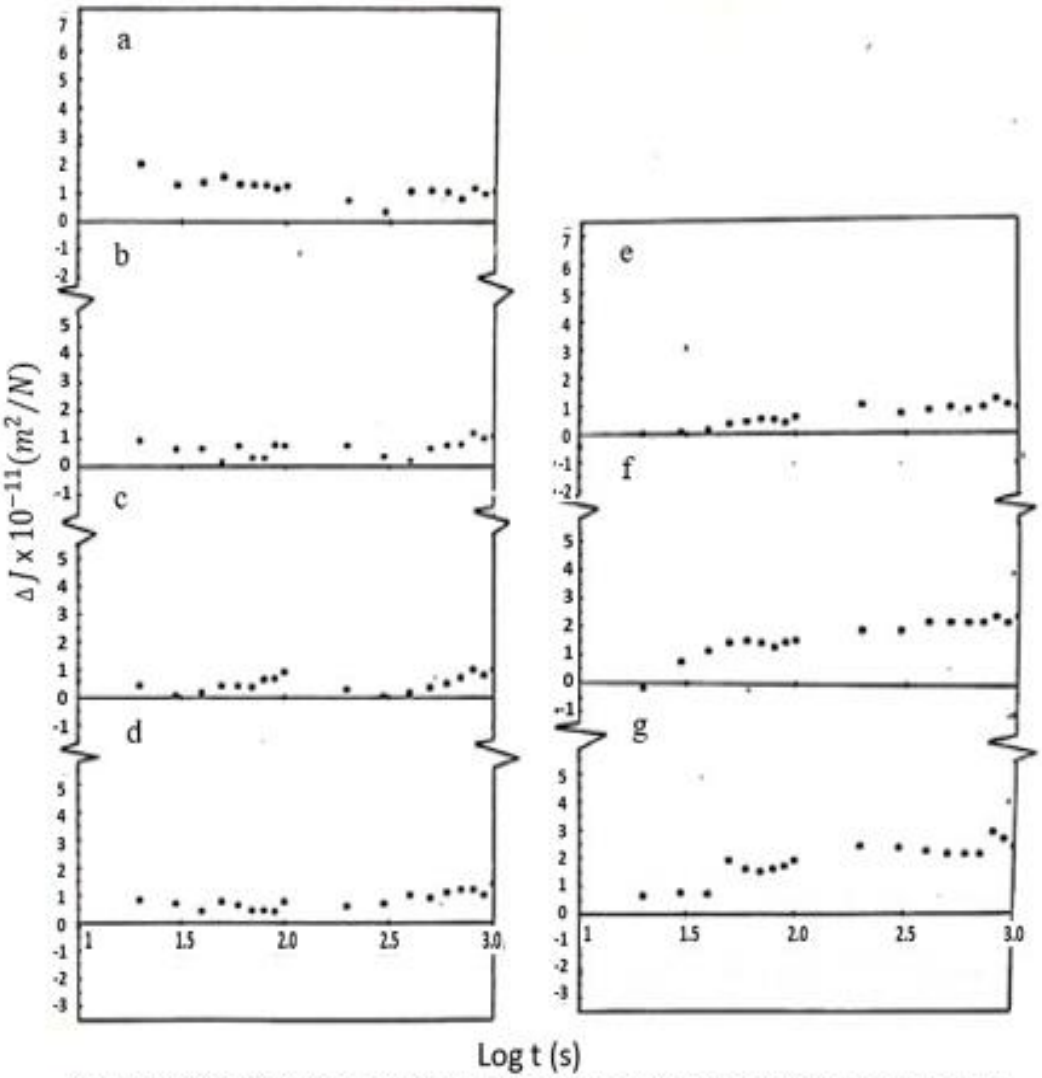

Fig. (4.15) The difference between creep and recovery shear Compliance J_c and J_r as a function of time at constant $I_1 = 5.477(MN/m^2)$ and varying $I_2{}' = 25(a), 50(b), 100(c), 150(d), 200(e), 250(f), 300(g)(MN/m^2)^2$ $(T = 30 \pm 0.2C^2)$

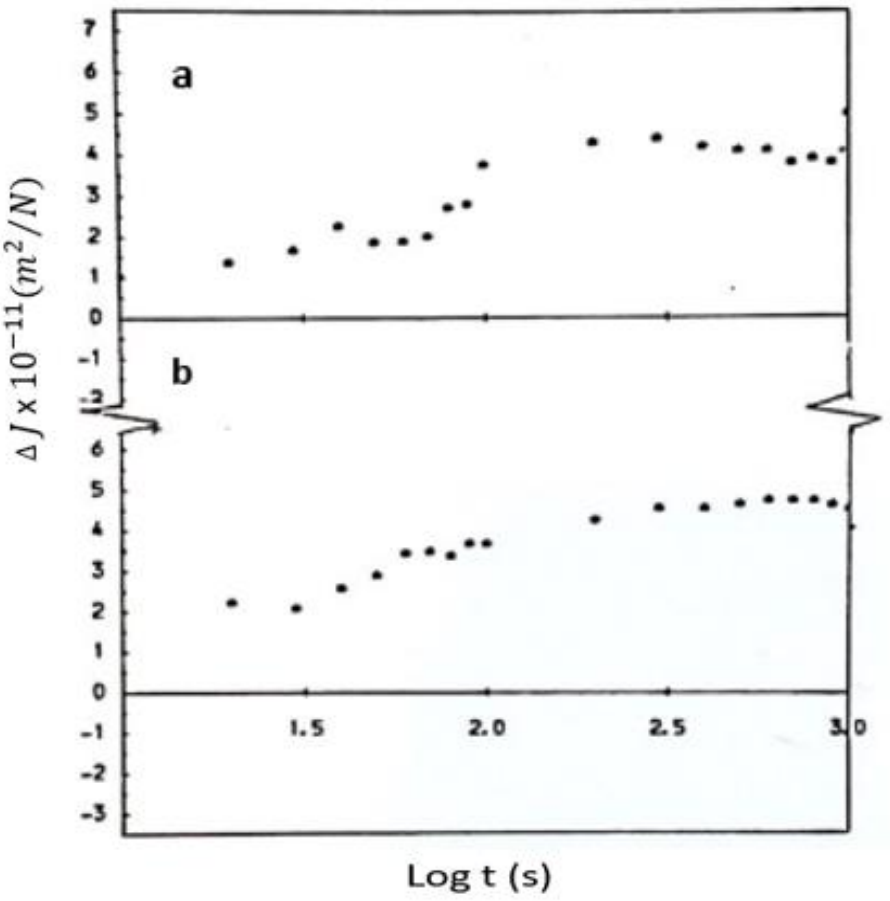

Fig. (4.16) The difference between creep and recovery shear Compliance J_c and J_r as a function of time at constant $I_1 = 0$ and varying $I_2' = 300(a), 400(b)(MN/m^2)^2$ $(T = 30 \pm 0.2C^2)$

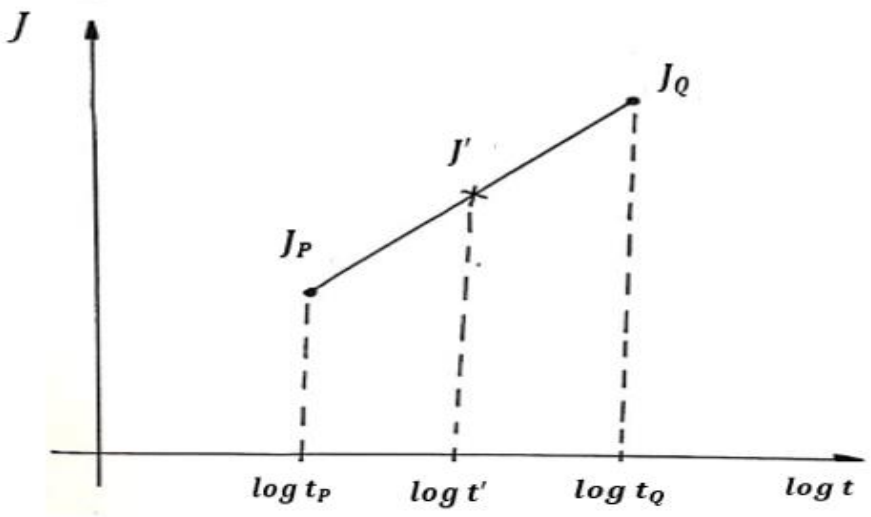

Fig. (4.17) Schematic diagram for the interpolation of J values.